Marine Pollution Bulletin 150 (2020) 110778

Contents lists available at ScienceDirect

Marine Pollution Bulletin

journal homepage: www.elsevier.com/locate/marpolbul

Variability of dinoflagellates and their associated toxins in relation with environmental drivers in Ambon Bay, eastern Indonesia

Sem Likumahua[a,b,*], M. Karin de Boer[a,c], Bernd Krock[d], Salomy Hehakaya[b], La Imu[b], Annegret Müller[d], Thomas Max[d], Anita G.J. Buma[a]

[a] Department of Ocean Ecosystems, Energy and Sustainability Research Institute Groningen, Faculty of Science and Engineering, University of Groningen, Nijenborgh 7, 9747AG Groningen, the Netherlands
[b] Centre for Deep Sea Research-LIPI, Jl. Y. Syaranamual Guru-guru Poka, 97233 Ambon, Indonesia.
[c] Beta Science Shop, Faculty of Science and Engineering, University of Groningen, Nijenborgh 6, 9747AG Groningen, the Netherlands
[d] Alfred Wegener Institute, Helmholtz Centre for Polar and Marine Research, Am Handelshafen 12, 27570 Bremerhaven, Germany

ARTICLE INFO

Keywords:
Harmful algae
Toxic dinoflagellate
Gymnodinium catenatum
Dinophysis miles
Pectenotoxin-2
PSTs

ABSTRACT

The aim of the present work was to unravel which environmental drivers govern the dynamics of toxic dinoflagellate abundance as well as their associated paralytic shellfish toxins (PSTs), diarrhetic shellfish toxins (DSTs) and pectenotoxin-2 (PTX2) in Ambon Bay, Eastern Indonesia. Weather, biological and physicochemical parameters were investigated weekly over a 7-month period. Both PSTs and PTX2 were detected at low levels, yet they persisted throughout the research. Meanwhile, DSTs were absent. A strong correlation was found between total particulate PST and *Gymnodinium catenatum* cell abundance, implying that this species was the main producer of this toxin. PTX2 was positively correlated with *Dinophysis miles* cell abundance. Vertical mixing, tidal elevation and irradiance attenuation were the main environmental factors that regulated both toxins and cell abundances, while nutrients showed only weak correlations. The present study indicates that dinoflagellate toxins form a potential environmental, economic and health risk in this Eastern Indonesian bay.

1. Introduction

Harmful algal blooms (HABs) are a potential threat to marine environments worldwide, while affecting humans in terms of health and economic loss (Anderson et al., 2014; Glibert, 2016). The main vector of algal toxins to humans is shellfish (James et al., 2010; Reis Costa, 2016). Syndromes of human poisoning from shellfish consumption are derived from five types of shellfish toxicity, namely Paralytic Shellfish Poisoning (PSP), Diarrhoetic Shellfish Poisoning (DSP), Neurotoxic Shellfish Poisoning (NSP), Amnesic Shellfish Poisoning (ASP), and Azaspiracid Shellfish Poisoning (AZP). In the present study, we focused only on PSP and DSP toxins as well as on pectenotoxins (PTXs), since associated phytoplankton species are frequently observed in eastern Indonesian waters (monitoring results, data not published), but related toxin data were lacking for Ambon Bay and Eastern Indonesia at large.

Paralytic shellfish poisoning (PSP) has increased worldwide in recent decades (Anderson, 2009; Navarro et al., 2014). Paralytic shellfish toxins (PSTs) are a group of paralytic toxin compounds, produced by marine dinoflagellates such as *Alexandrium* spp. (*A. catenella*, *A. minutum*, *A. fundyense*), *Gymnodinium catenatum* and *Pyrodinium bahamense* (Etheridge, 2010; Ujevic et al., 2012; Xie et al., 2013; Burrell et al., 2013; Navarro et al., 2014). Based on the chemical structure and toxicity level, PSTs are divided into three groups: highly toxic carbamoyls (saxitoxin (STX), neosaxitoxin (NEO) and gonyautoxins (GTX1-4)), intermediate toxic decarbomoyls (dcSTX, dcGTX and dcNEO); and the least toxic N-sulfocarbamoyls (C1-4, B1 and B2) (Costa et al., 2010). Ingestion of PSTs by humans and marine mammals results in the blocking of voltage-gated sodium channels, leading to headache, nausea, vomiting, diarrhea, muscular paralysis and respiratory difficulty (Costa et al., 2010; James et al., 2010). Environmental factors, which have shown to influence PST production include temperature, salinity, light intensity, nutrient concentration and increased CO_2 (Tatters et al., 2013; Laabir et al., 2013). For Ambon Bay nothing was known about the potential threat for human consumption related to PSTs, but bloom proportions of *P. bahamense* had been recorded before which had caused serious health problems associated with shellfish consumption (Wiadnyana et al., 1996; Likumahua, 2013),

Proliferations of the dinoflagellate genus *Dinophysis* Ehrenberg are

* Corresponding author at: Department of Ocean Ecosystems, Energy and Sustainability Research Institute Groningen, Faculty of Science and Engineering, University of Groningen, Nijenborgh 7, 9747AG Groningen, the Netherlands.
E-mail address: s.likumahua@rug.nl (S. Likumahua).

https://doi.org/10.1016/j.marpolbul.2019.110778
Received 12 June 2019; Received in revised form 21 November 2019; Accepted 23 November 2019
Available online 04 December 2019

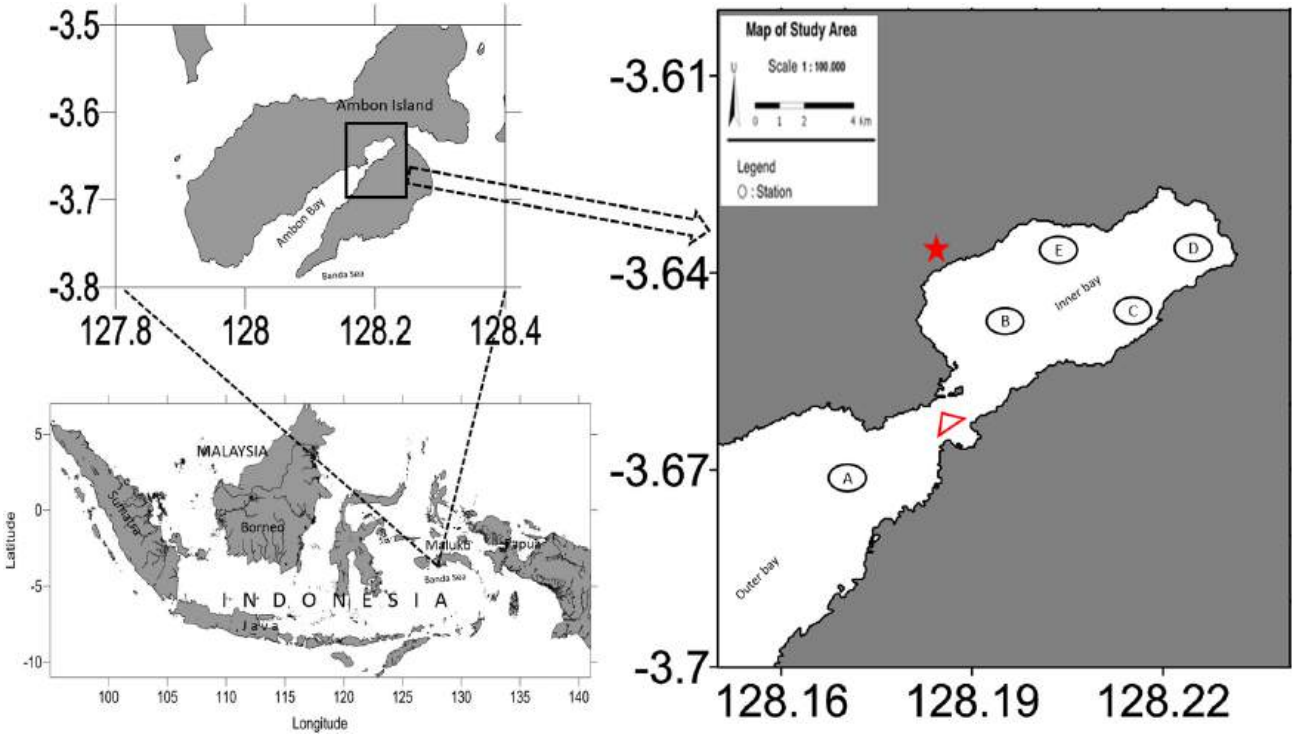

Fig. 1. Map of Ambon Bay with the location of the five sampling stations (A–E). The red star shows the location of LIPI, the Centre of Deep Sea Research in Indonesia, the red triangle shows the location of the sill. (For interpretation of the references to color in this figure legend, the reader is referred to the web version of this article.)

associated with diarrhetic shellfish poisoning (DSP) events. These cause major problems in shellfish industry and public health around the world (Lindahl et al., 2007; Pizarro et al., 2009). The genus is able to produce diarrhetic shellfish toxins (DSTs) such as okadaic acid (OA) and dinophysistoxins (DTXs) as well as pectenotoxins (PTXs) as secondary metabolites, which accumulate in filter feeders, leading to human poisoning and symptoms of nausea, vomiting, diarrhea, chills and abdominal pain (Pizarro et al., 2008; Hess, 2010; Li et al., 2014; Reguera et al., 2014; Hu et al., 2017). PTXs were formerly grouped in the DSP toxin complex. Yet, as recently shown, PTXs do not reveal diarrhea symptoms after oral administration to laboratory rodents (Fabro et al., 2016). As a result, PTXs are now excluded from the DST group.

Twelve *Dinophysis* species (*D. ovum*, *D. acuta*, *D. acuminata*, *D. fortii*, *D. caudata*, *D. sacculus*, *D. miles*, *D. norvegica*, *D. rotundata*, *D. mitra*, *D. infundibulus*, *D. tripos*) have been confirmed to contain DSTs (MacKenzie et al., 2005; Miles et al., 2006; Fernández et al., 2006; Blanco et al., 2007; Lindahl et al., 2007; Pizarro et al., 2008; Suzuki et al., 2009; Fabro et al., 2016). Yet, only the first seven of them were found to be associated with DSP events (Reguera et al., 2012). Blooms of *D. caudata* have often been found to co-occur with other *Dinophysis* species such as *D. acuminata* and *D. miles* (Marasigan et al., 2001; Reguera et al., 2012; Reguera et al., 2014). Yet, very little is known about *D. miles* since only one study has been done on the species (Marasigan et al., 2001). The toxin production of *Dinophysis* is influenced by a combination of genetic and environmental factors, resulting in species and location specific variability in toxin profiles and cell quotas (Mafra et al., 2014). In addition, culture experiments revealed that cell growth phase was the main factor regulating toxin production and content, which varied among strains (Reguera et al., 2014).

Indonesian waters have experienced increased HABs in recent decades, resulting in environmental and economic problems, as well as human illness (Aditya et al., 2013). In the densely populated Ambon Bay, in the eastern part of the country, human illness and fatalities have been recorded in 1994 and 2012 due to toxic-dinoflagellate proliferations, dominated by *P. bahamense* (Wiadnyana et al., 1996; Likumahua, 2013). Since then, phytoplankton abundance, and especially potentially toxic species are monitored in the area by a monthly-based program. Other potentially toxic dinoflagellate species frequently observed in phytoplankton samples include *Dinophysis* spp., *Gymnodinium catenatum*, and *Alexandrium* spp., (monitoring results, data not published). Up to now, no studies had been carried out to detect the toxins associated with these dinoflagellate species, in Ambon Bay and other Indonesian waters. In addition, no effort had been made to explain species dynamics as a function of environmental variability. As a result, this complete lack of information hampered the establishment of a suitable HAB management program nationwide. Thus, the present study was designed to investigate dynamics of potentially toxic dinoflagellates as well as their associated toxins, in relation with environmental conditions in Ambon Bay, Eastern Indonesia. To this end, a seven-month field research was carried out in the bay, during which biological data were collected in conjunction with relevant physico-chemical and weather data.

2. Materials and methods

2.1. Study area and sampling

Ambon Bay is a semi-enclosed estuary located in Ambon City, the capital of Maluku Province, eastern Indonesia. A narrow and shallow sill (Fig. 1 and Supplementary materials Fig. S1) divides the bay into an inner and outer bay, and restricts water circulation to the open ocean. The area is subjected to a tropical climate with two main seasons. The dry season is associated with the northwest monsoon occurring between October and March, and is characterized by low precipitation and relatively high air temperatures. The wet season is characterized by high precipitation and relatively low air temperatures, occurring during the southeast monsoon between March and September. The period of transformation from the dry to wet season is known as Transition I (between March and May), and from the wet to dry season is Transition

II (between September and November).

In the inner bay, four sampling stations (B, C, D and E) were selected, while a reference station (A) was chosen in the outer bay, reflecting a higher oceanic influence (Fig. 1). Stations C and D are located near dense mangrove vegetation and small river outflows. Stations B and E are located close to river outflows, which massively flush surrounding agricultural and human wastewater into the inner bay during the wet season. Some fish farms are located in the inner bay, close to stations C, D and E. Two massive dinoflagellate blooms were recorded in the area around stations C and D during the wet seasons of 1994 and 2012. Meanwhile, a proliferation of dinoflagellates was recorded during the dry season around stations B and E in 2013. These blooms were dominated by the toxic *P. compressum* (Wiadnyana et al., 1996; Likumahua, 2013).

Weekly field sampling was carried out at these five stations between January and July 2018 throughout the dry and wet season. In order to follow the former dinoflagellate bloom periods, samples were collected twice a week during the peak of both the dry (February–March) and wet (June–July) season. Thus, sampling was done 42 times resulting in 210 samples taken in total during the research. The period between the end of March and mid-May was considered as the transition (phase I) from the dry to wet season. The total time spent for boating and sampling was between 2 and 2.5 h, prior to sample processing in the Centre for Deep Sea Research (CDSR) - LIPI laboratories.

2.2. Weather and water column properties

A weather station was installed at the LIPI institute (Fig. 1) to continuously record precipitation, air temperature, humidity and wind speed (15 min frequency). Data were calibrated with the data recorded by the local Meteorological and Climate Bureau. For the statistical analysis, the average of 12 h prior to sampling was calculated for precipitation and wind speed. A compact Alec CTD Model ASTD 687 was deployed to measure depth, temperature, salinity, turbidity, density and chlorophyll-a (Chl-a) fluorescence. Temperature and density profiles were used to calculate mixed layer depth (MLD) and stratification indices using the threshold method as described by González-Pola et al. (2007) and Somavilla et al. (2017). At depths 1, 2, 4, 6, 8, 10, 12, 16, and 20 (m), irradiance attenuation was measured using a LiCor Li1400 light meter. Data were log transformed to calculate the light extinction coefficient (kd). Tidal elevation data were obtained from the Hydrography and Oceanography Centre, Indonesian Navy.

2.3. Nutrient sampling and analysis

Water samples were collected with a 3.5 L Niskin bottle at two depths, representing water layers above (2 m) and below (20 m) the thermocline, if present. Water was pre-filtered on board using a 20 μm filter mesh to eliminate large plankton, organic material and sediment particles. Filtered water samples were transferred to pre-cleaned (Milli-Q water) 600 mL bottles and stored in a dark insulated box, filled with seawater at ambient-temperature. In the lab, samples were filtered immediately through 0.2 μm pore size, 47 mm Ø Fisherbrand nylon membrane filters using a vacuum pump with 0.3 bar maximum pressure, and stored at −20 °C until analysis. Dissolved nutrients, Nitrate (NO_3), Phosphate (PO_4) and Silicate (SiO_2) were measured using a spectrophotometer (UV–Vis Shimadzu 1700) following Strickland and Parsons (1972), and Ammonium (NH_4) following APHA (1998).

2.4. Chl-a and cell abundance

Phytoplankton samples were collected from the upper 20 m using a Hydro-bios plankton net (Ø 40 cm, length 100 cm, 20 μm mesh size). The net was deployed twice vertically at a constant pulling speed, following the manufacturer's guidelines. Samples were transferred to 500 mL bottles and adjusted to a final volume of 400 mL with filtered seawater, and kept at ambient temperature in the dark in an insulated box.

For microscopic inspection and cell counting, 40 mL of sample was fixed with acidic lugol iodine solution and a drop of formalin (4% final concentration) to inactivate bacteria. The fixed samples were kept in the dark at 4 °C until sample analysis. Ten milliliter Uthermöhl chambers were used to sediment cells for at least 12 h prior to inspection at 200× magnification using an Olympus LH 50A inverted microscope. Since dinoflagellate abundance was generally low, cell counts were done in the whole chamber, after which final cell density was expressed in cells per net tow (cells NT^{-1}).

For chlorophyll-a analysis, 60 mL of the concentrated net samples were filtered through 25 mm Ø GF/F Whatman filters using a vacuum pump with a maximum pressure of 0.2 bar. Filters were transferred to darkened glass tubes filled with 10 mL of 90% acetone. After mixing, the samples were kept at 4 °C in a refrigerator. After a few hours, the filters were ground to optimize extraction efficiency using a mini glass spatula and subsequently refrigerated overnight. Samples were centrifuged for 8 min at 8400 ×*g*, and measured in a spectrophotometer (UV–Vis Shimadzu 1700) at wavelengths of 750, 665, 645 and 630 nm. Chlorophyll-a (Chl-a) was calculated using the equations as described by Strickland and Parsons (1972).

2.5. Toxin analysis

Liquid chromatography – tandem mass spectrometry (LC-MS/MS) was used to detect PSTs (C1/2, dcGTX2/3, GTX2/3, GTX1/4, B1, dcSTX, STX, and NEO), DSTs (okadaic acid (OA), DTX1, and DTX2) and PTXs according to Krock et al. (2008). For each toxin group, 100 mL of net sample was concentrated by centrifugation at 12,100 ×*g* for at least 20 min and transferred to 2 mL Eppendorf tubes. Pellets were then stored at −20 °C prior to analysis. Approximately 0.9 g lysing matrix D was added to the pellets followed by 500 μL solvent (methanol for DSTs and PTXs, while 0.03 M acetic acid for PSTs). Toxin extraction was performed at maximum speed (6.5 m s^{-1}) for 45 s using a Bio101 FastPrep (Thermo Savant, Illkirch, France). Homogenized samples were centrifuged at 16,100 ×*g* at 4 °C for 15 min, after which the supernatants were transferred to 0.45 μm pore size spin filters (Milipore Ultrafree, Eschborn, Germany) and centrifuged for 30 s at 5700 ×*g*. Filtrates were transferred to HPLC vials for toxin analysis, expressed in ng NT^{-1}. Analysis was done following Krock et al. (2008) and detection limits for each toxin were determined (Table 1). Toxin cell quotas of dominant species were calculated according to ICES (2006) recommendations, and thereby only applied to cell abundances higher than 10,000 cells NT^{-1}.

Table 1
Limit of detection (LoD) for each PSTs, DSTs and PTX2.

PSTs	LoD	DSTs and PTX2	LoD
	ng NT^{-1}		ng NT^{-1}
C1	0.5	OA	5.91
C2	0.08	DTX1	2.94
dcGTX2	2.13	DTX2	3.23
dcGTX3	0.16	PTX2	0.37
GTX2	0.11		
GTX3	0.08		
GTX1	0.52		
GTX4	0.39		
B1	0.12		
dcSTX	0.43		
STX	0.02		
NEO	0.17		

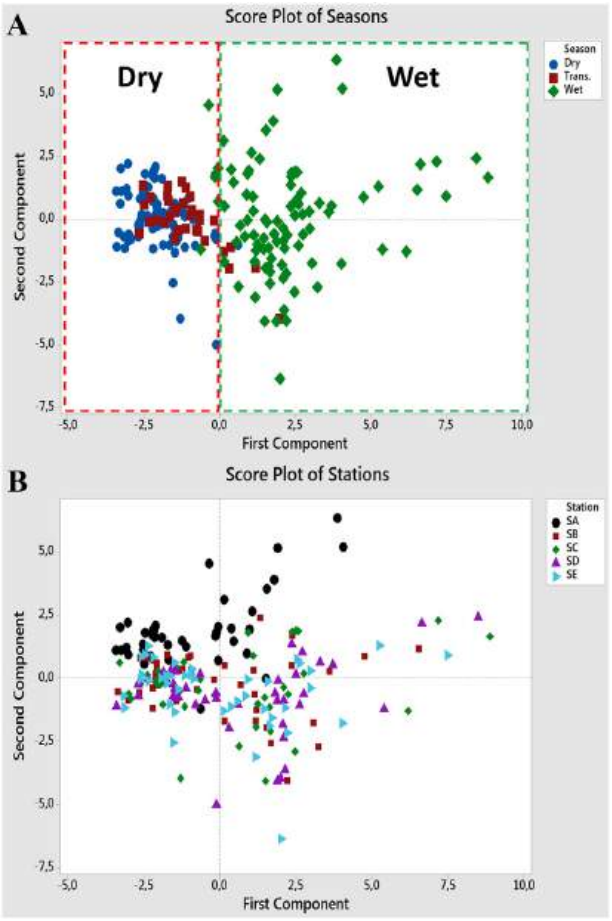

Fig. 2. PCA analysis of all weather, water properties and biological data of Ambon Bay in 2018. A: score plot for seasons and B: score plot for stations (n = 210).

2.6. Statistical analysis

Statistical analysis was done using the Minitab 18 package. A Principal Component Analysis (PCA) was performed to investigate the grouping among stations and seasons, based on all data (weather, physicochemical and biological data). Relationships between environmental parameters and biological variables were measured using a non-parametric Spearman's rank correlation. The relationship between total PST levels and *G. catenatum* cell abundances was established using the parametric Pearson's correlation since the data were normally distributed.

3. Results

3.1. Season and station plots

The PCA score plot analysis of all parameters revealed a clear separation between the two main seasons, dry and wet (Fig. 2A). In addition, the transition period showed similar traits with the dry season. Exceptions were observed for four points of the transition period ending up in the wet season cluster, implying that these data share similar characteristics with the wet season. Since these data belonged to the days when the wet period had just started, they were grouped in this season. Based on these results, the separation of the transition period between the dry and wet season was defined on day 120 (end of April). The other score plot analysis showed a little deviation of station A in the outer bay from stations in the inner part (Fig. 2B). Thus, spatially, no clear separation was found among stations.

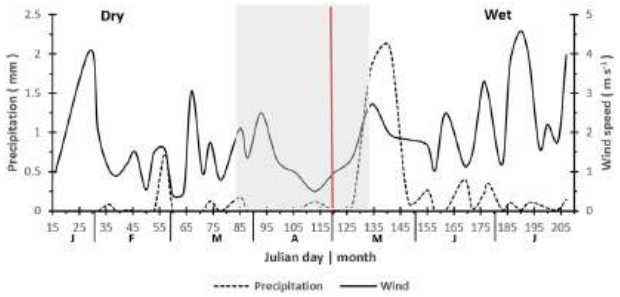

Fig. 3. Weather conditions recorded as average values for 12 h prior to sampling. The grey area refers to the transition period between dry and wet season. The vertical red line separates the two distinct seasons, as determined by statistical PCA analysis of environmental conditions in Ambon Bay 2018. (For interpretation of the references to color in this figure legend, the reader is referred to the web version of this article.)

3.2. Weather variability

The 12 h averages for precipitation showed low intensities during the dry season, with only six rainy days, ranging between 0.01 and 0.7 mm of the total daily rate. High rates and more frequent precipitation intensities were recorded during the wet season. Two high precipitation days (1.8 and 2.1 mm total daily rate) were found at the start of the wet season between day 127 (early May) and 148 (end of May) (Fig. 3). High wind speeds were recorded at the beginning of the year between day 16 (mid of January) and 36 (early February), with average velocities between 1.1 and 4.1 m s^{-1}. A stable trend was recorded during the rest of the dry season, followed by a gradual decrease during the transition period. In the wet season, the average wind speed showed an upward trend with a gradual increase and a maximum velocity of 4.6 m s^{-1} (Fig. 3).

3.3. Physicochemical properties

Average (0–20 m) water temperatures decreased during the observation, reaching lowest levels during the wet season. A slightly increasing trend was recorded in the dry season reaching a maximum of 30 °C and the lowest temperature (26.6 °C) was found at the end of the wet season (Fig. 4A). Station D had the highest water column temperature (30.2 °C, day 78 (mid of March)), and station A had the lowest temperature (day 141 (mid of May)) (Supplementary materials Fig. S2A). During the dry season, the shallow Station D was warmer than the other stations, however this station was cooler during the subsequent wet season. On average, the deepest station A had the lowest water column temperature compared to the other stations. Contrary to temperature, the average salinity level showed an upward trend in spite of a disruption by a slight gradual downward trend between the middle and end of the dry season (Fig. 4A). The salinity ranged between 32.9 and 33.5 (Fig. 4A). The highest salinity was recorded at station A (day 197 (mid of July)) and the lowest on day 141 (second half of May) at station E (Supplementary materials Fig. S2B).

Tidal elevation increased during the observation, yet showed high variability over time due to differences in the tidal cycle during sampling, ranging between 0.2 and 1.9 m (Fig. 4B). From the overall station profiles, high elevation values were found at station E and low values at station A (data not shown). Mixed layer depth (MLD) was highly variable in space and time, revealing unclear patterns (Fig. 4B). Shallow MLDs roughly occurred above 10 m depth at stations located in the inner bay during the wet season. Meanwhile, deep MLDs were recorded at station A ($>$ 15 m depth) (Supplementary materials Fig. S2D). During the dry season, the stratification index was found to be below 1.0 kg m^3, increasing to 2.9 kg m^3 on day 190 (early July) (Station E) in the wet season. The water column in the inner bay was much more stratified than in the outer bay (Station A: $\leq$0.5 kg m^3), which showed

the lowest stratification index throughout the sampling period (Supplementary materials Fig. S2E). Irradiance attenuation (kd) increased during the observation, despite a stable and a slightly downward trend during the second half of the dry season (Fig. 4C). Highest kd coefficients were found at station C (0.37) and station D (0.38), while station A had lowest values (Supplementary materials Fig. S2C).

Surface (2 m) phosphate concentration were on average lower than at 20 m, ranged between 0 and 3.0 μM and showed a high temporal and spatial variability (Supplementary materials Fig. S3A). Silicate showed an upward trend throughout the sampling period, yet concentrations above the thermocline at 2 m (≥10 μM) were higher than those at 20 m (≤10 μM) (Supplementary materials Fig. S3C & D). Similarly, nitrate concentrations showed upward trends at both depths, ranging between 0.01 and 3.0 μM. Highest average nitrate concentrations were found below the thermocline (Supplementary materials Fig. 3E & F). Ammonium increased throughout the sampling period despite a sharp decrease in the middle of the wet season (Supplementary materials Fig. S3G & H). Ammonium concentration ranged between 0 and 16 μM. Overall nutrient data showed that the inner bay stations experienced higher nutrient loadings than station A in the outer bay. Yet, ammonium concentrations were comparable for all stations. (Supplementary materials Fig. S3G & H).

3.4. Chl-a, dinoflagellate abundances and toxin variability

Chl-a was measured with a fluorescence sensor mounted on the CTD as well as in net samples that reflected the phytoplankton cell fraction ≥ 20 μm. These two chl-a data sets showed a strong correlation ($r = 0.8$ and $p = 0.000$). As a result, only the net fraction data were further considered, given their direct comparison with cell abundance and toxin results, obtained from the same net hauls. Chl-a levels revealed an upward trend during the sampling period, reaching maximum levels in the wet season (Fig. 4C). The average-station levels ranged between 0.01 and 1.0 mg m^{-3}. Spatially, highest chl-a levels were found at the inner bay stations (data not shown).

Dinoflagellate communities were dominated by the genera *Gymnodinium, Ceratium, Dinophysis* and *Alexandrium*. PST producing species were dominated by *G. catenatum* (Supplementary materials Fig. S4D) and *Alexandrium* spp. Abundances of *Alexandrium* spp. varied over time and ranged between not observed and 3.5 × 10^3 cells NT^{-1}. Lowest abundances were found during the dry season and subsequently increased during the wet season, thus overall showing an upward trend (Fig. 5A). Spatially, this genus was found in highest densities at the inner bay stations. Likewise, *G. catenatum* was found in low densities during the dry season, and subsequently reached peaks during the wet period (Fig. 5B). Thus, its overall abundance showed a clear upward trend, ranging between not observed and 40 × 10^3 cells NT^{-1}. Highest abundances were found in the inner bay, mostly at stations D and B (Fig. 5B). Although both PSP genera increased during the wet season, their peak abundances did not follow similar patterns.

Generally, DST producing species belonged to the genus *Dinophysis*: *D. miles*, *D. caudata* and *D. acuminata* (Supplementary materials Fig. S4A–C). Other species like *D. norvegica* and *D. tripos* were scarcely found and occurred in very low abundances. Cells of *D. caudata* and *D. acumintata* were found in respectively 24% and 13% of the total amount of samples ($n = 210$). Cell abundances of *D. caudata* ranged from not observed to 1.8 × 10^3 cells NT^{-1}, *D. acuminata* from not observed to 280 cells NT^{-1}. Abundance maxima of both species were mostly recorded during the wet season, however with some pronounced peaks in the dry period at station A (Fig. 6A & B). Cell abundances of *D. miles* were higher than two other species, ranging between not observed and 14.2 × 10^3 cells NT^{-1}. The abundance showed a clear upward trend with abundance maxima recorded during the wet season (Fig. 6C). A distinct spatial distribution was also shown for *D. miles*, which mostly occupied stations in the inner bay, especially C and D. The three *Dinophysis* species therefore showed different abundance patterns, both in space and in time (Fig. 6).

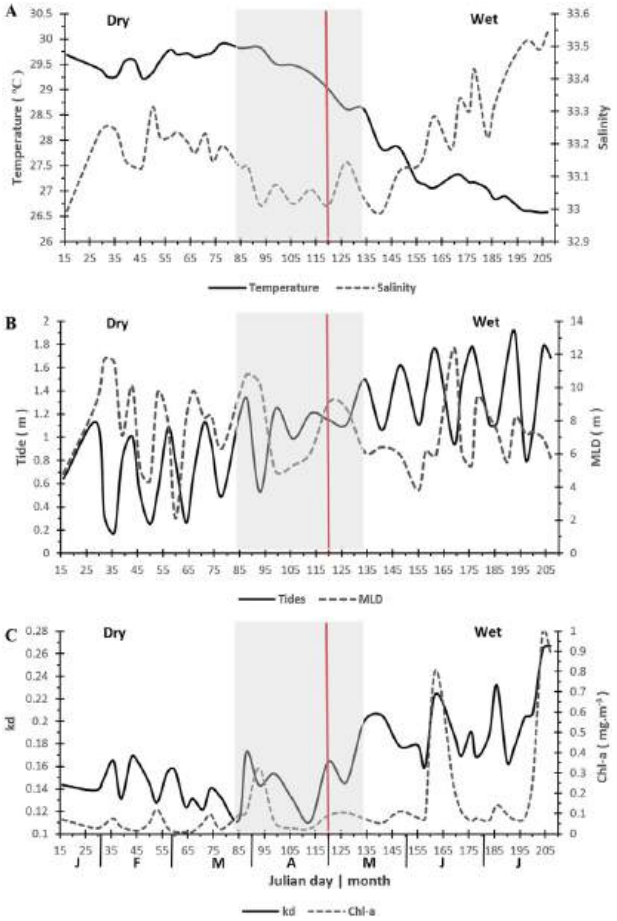

Fig. 4. Temporal variability (average value of the five stations) of water physical properties and Chl-a. A: average 0–20 m temperature and salinity, B: tide elevation and mixed layer depth (MLD), and C: Irradiance attenuation (kd) 0–20 m and Chlorophyll-a net (cell fraction ≥ 20 μm). The grey area refers to the transition period between dry and wet season. The vertical red line separates the two distinct seasons, as determined by statistical PCA analysis of environmental conditions in Ambon Bay 2018. (For interpretation of the references to color in this figure legend, the reader is referred to the web version of this article.)

Tandem mass spectrometry revealed a profile of PSTs constituted by N-sulfocarbamoyl, decarbamoyl and carbamoyl components. In samples where *G. catenatum* was found in high abundances, eight PST analogues were detected. Decarbamoyl (dcGTX2-3 and dcSTX) and N-sulfocarbamoyl (C1-2) dominated the PST profiles, while the highly toxic carbamate group (GTX2-3 and STX) showed low levels (Table 2). Since some PSTs were almost always detected at very low levels, PST data were pooled together, leading to an overall PST estimate. The PSTs level increased during the wet season and continued to decrease rapidly in the dry period, leading to low levels around the limit of detection (LoD) (Fig. 7A). Relatively high levels were found at the beginning of the wet season between days 120 (end of April) and 134 (mid of May), at stations C and D. PST levels ranged between 4.71 and 1380 ng NT^{-1}. As for the dominant species *G. catenatum*, the toxin cell quota ranged between 0.01 and 0.04 ng PST $cell^{-1}$ ($n = 6$). Okadaic acid (OA) was scarcely detected above LoD, thus, it was not further considered in this study. As for the *Dinophysis* toxins, DTX1 and DTX2 were absent in the phytoplankton samples. Yet, PTX2 and its seco-acid PTX2sa were successfully detected above the LoD, implying that *Dinophysis* in Ambon Bay was associated with these toxins. However, only 10% of the 210 samples contained PTX2sa. As a result, PTX2sa was not described further and excluded from the statistical analysis. PTX2 was recorded to be

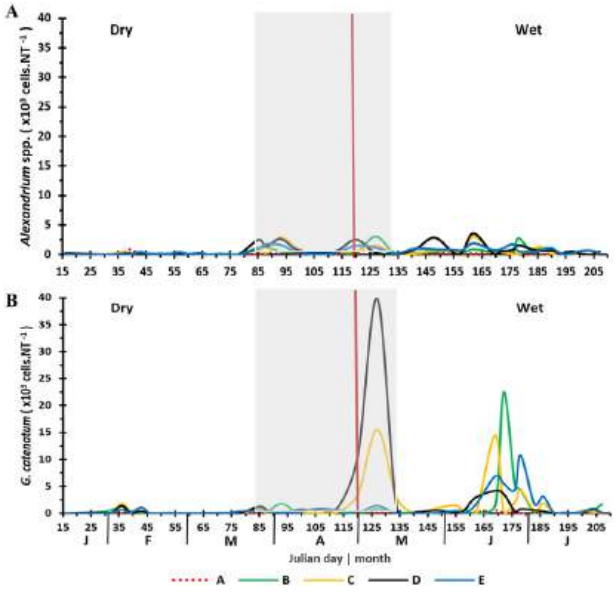

Fig. 5. Temporal variability of PST producing species for the five sampling stations. The grey area refers to the transition period between dry and wet season. The vertical red line separates the two distinct seasons, as determined by statistical PCA analysis of environmental conditions in Ambon Bay 2018. (For interpretation of the references to color in this figure legend, the reader is referred to the web version of this article.)

highly variable, yet it showed a clear upward trend over time. PTX2 levels were very low during the dry season but increased during the second half of the dry season into the wet season (Fig. 7B). PTX2 levels ranged between not detectable and 26 ng NT^{-1}. PTX2 cell quota for the dominant species *D. miles* was calculated to be 0.87 pg PTX2 $cell^{-1}$ ($n = 1$).

3.5. Relationship between dinoflagellates, toxins and environmental factors

Spearman rho analysis revealed a strong correlation between the total PST level and *G. catenatum* abundance both throughout the observation and during the wet season ($r = 0.95$ and 0.7; $p = 0.000$, respectively) (Table 3). In addition, regression analysis between *G. catenatum* abundances and PST levels showed a strong positive correlation (Fig. 8). Similarly, Spearman rho analysis showed a positive correlation between *Alexandrium* spp. and the total PST level ($r = 0.4$; $p = 0.000$), yet it was much weaker than for *G. catenatum*. High cell densities of *G. catenatum* and PST levels were found on day 127 (early May) at stations D and C (Table 2; Figs. 5B and 7A). On this day, *Alexandrium* spp. densities were found to be 10 to 100 times lower than *G. catenatum* (Table 2). Meanwhile, no *P. compressum* cells were observed in these samples. During the wet season, temperature significantly correlated with the total PST level as well as their associated species, while nutrients showed slightly negative correlations (Table 3).

Over the whole sampling period, positive weak correlations were found among PTX2 and *D. miles* as well as chl-a ($r = 0.5, p = 0.000$). At the peak of highest PTX2 on day 141 (second half of May) at stations B and E, cell abundances of *D. miles* were 1.48×10^3 and 1.34×10^3 cells NT^{-1}, respectively (Figs. 6C and 7B). Meanwhile, cells of the other two species were not observed (Figs. 6A & B and 7B). Similarly, another peak of PTX2 on day 134 (mid of May) at station C, coincided with a *D. miles* abundance of 0.74×10^3 cells NT^{-1} while cells of the two other species were absent. Various environmental factors showed positive correlations with PTX2 including water properties (MLD, stratification, kd and tide), nutrients and precipitation (Table 3). Physical factors such as MLD, stratification, kd and tide governed the abundance of *D. miles*, meanwhile, nutrients showed weak correlations.

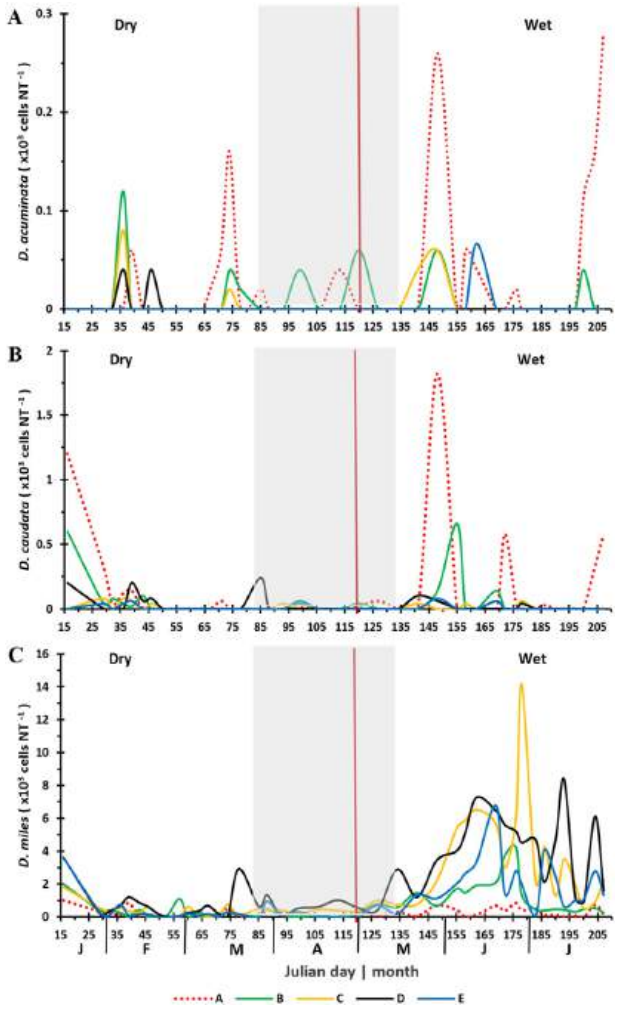

Fig. 6. Temporal variability of DST and PTX producing species for the five sampling stations. The order of graphs is arranged from the lowest to highest abundance species (note differences in scales). The grey area refers to the transition period between dry and wet season. The vertical red line separates the two distinct seasons, as determined by statistical PCA analysis of environmental conditions in Ambon Bay 2018. (For interpretation of the references to color in this figure legend, the reader is referred to the web version of this article.)

During the wet season, no environmental driver revealed a clear correlation with the toxin, yet, kd, phosphate and nitrate level at 20 m were found to correlate with *D. miles* abundance (Table 3).

4. Discussion

Throughout the seven-month research in Ambon Bay, both PSTs and PTX2 as well as their associated dinoflagellate species were successfully detected. Meanwhile, DSTs were not detected. As a result, this study provides the first evidence of PSTs and PTX2 persistence in Indonesian waters as well as a first insight in their seasonal variability as a function of environmental drivers.

4.1. Environmental dynamics

Seasonal monsoons that characterize the tropical climate in Ambon Island have effects on physicochemical properties in the bay. Upwelling (southeast monsoon, the wet season) and down-welling (northwest monsoon, the dry season) events in the Banda Sea massively influence surrounding nearshore waters including Ambon Bay (Wyrtki, 1961;

Table 2
PST profiles from two samples of the highest Gymnodinium catenatum abundance.

Samples	Toxin profiles and levels in ng NT^{-1}					G. catenatum	Alexandrium spp.
	C1/2	**dcGTX2/3**	**GTX2/3**	**dcSTX**	**STX**	10^3 cells NT^{-1}	10^3 cells NT^{-1}
Day 127 Station C	332.35	223.34	2.04	7.82	5.80	15.60	1.54
Day 127 Station D	767.93	579.02	5.99	16.39	10.12	39.76	0.32

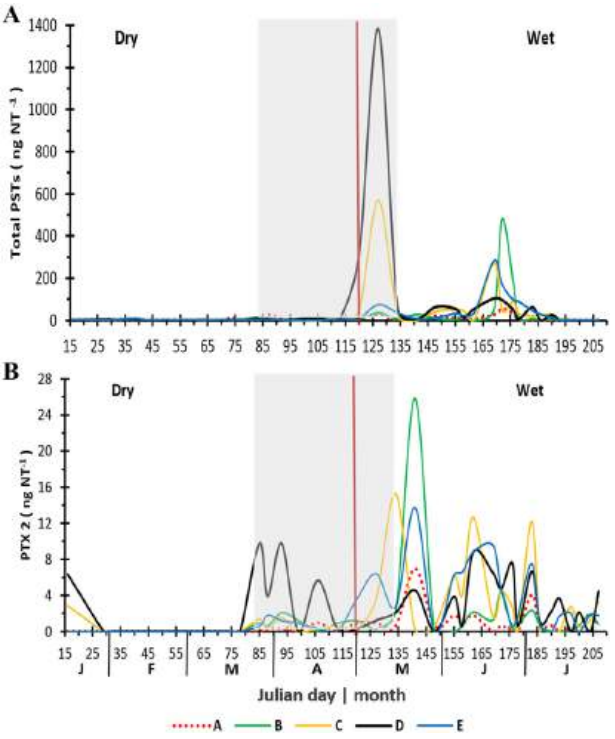

Fig. 7. Temporal variability of the total PSTs (A) and PTX2 (B) levels for the five sampling stations. The grey area refers to the transition period between dry and wet season. The vertical red line separates the two distinct seasons, as determined by statistical PCA analysis of environmental conditions in Ambon Bay 2018. (For interpretation of the references to color in this figure legend, the reader is referred to the web version of this article.)

Boëly et al., 1990; Zijlstra et al., 1990). During the wet season, relatively low water temperatures coupled with high salinities were detected for all five stations in Ambon Bay, reflecting upwelling properties in the Banda Sea (Fig. 4A). Here, upwelled-nutrient rich water from 20 m or deeper could be detected as a result of tidal forcing, replacing approximately 70% of the local water masses in the inner bay (Saputra and Lekalette, 2016; Corvianawatie et al., 2014). On average, wind speed influenced mixed layer depth in the inner bay during the dry season (Fig. 3 and Supplementary Fig. S2D), yet showed no effects during the wet season. Instead, increased precipitation enhanced irradiance attenuation, which was stimulated by massive runoff of highly turbid water and water column stratification during the wet period.

High wind speeds at the beginning of the year triggered water mixing in the inner bay, which may have resulted in elevated nutrient concentrations between January (day 23) and February (day 33) during the dry period (Fig. 3 and Supplementary Fig. S3). The overall trend showed further nutrient enhancement during the wet season, most clearly for nitrate, ammonium and surface silicate, which might be due to massive runoffs (Supplementary Fig. S3). A similar trend was reported in the LIPI monitoring program between 2012 and 2015 (data not published). Judging from statistical analysis, increased nutrient concentration was not strongly regulated by precipitation and associated runoffs (data not shown). This would imply that precipitation only partly served as an environmental driver. However, unknown and variable time delays between precipitation and runoff may have contributed to this relative mismatch. In addition, deep nutrient rich upwelled water from the Banda Sea, coupled with a short residence time of approximately 14 days might contribute further to the elevated nutrient levels during the southeast monsoon period as suggested before (Ikhsani et al., 2016). Hence, generally, land inputs through runoffs might dominate eutrophication during high precipitation years, whereas upwelling effects might dominate during low rate precipitation years.

4.2. PST and associated species

Overall dinoflagellate abundances were low throughout the research and no blooms were recorded, yet potentially toxic dinoflagellates occurred persistently, reaching highest cell densities during the wet season. The dominant dinoflagellate species found in our study are highly similar with the monitoring data generated from Ambon Bay since 2008. Yet, in earlier years, the toxic species *P. bahamense* was frequently observed, especially between June and July during the southeast monsoon (LIPI monitoring program, not published; Likumahua, 2013). In this study, PST producing *P. bahamense* cells were rarely observed and *Alexandrium* spp. showed low densities only throughout the research. The non-toxic *Alexandrium affine* was found to form a bloom in the bay earlier in 1997, and frequently occurred in phytoplankton samples (Wagey, 2002). Yet, in the present study, we also encountered cells of *Alexandrium* cf. *tamiyavanichii* and other *Alexandrium* species, although in very low cell numbers. Given the difficulty in determining toxic *Alexandrium* species especially in very low cell numbers, the species abundance was pooled as *Alexandrium* spp. Thus, contributions of this species on the PST level might be low.

A strong correlation between *G. catenatum* abundances and PST levels revealed a potential source of the toxin other than *P. compressum* in the area. The presence of *G. catenatum* was frequently recorded before, for example during campaigns in 1997–1998, four years after the major PSP event in Ambon Bay (1994) caused by *P. compressum* (Wagey, 2002). Thus, it is likely that Ambon Bay can be subject to future PSP events caused by *G. catenatum*. This species is so far known as the only PST producer in the gymnodinoid dinoflagellate group (Hallegraeff and Fraga, 1996). Human fatalities, fish and shrimp mortalities were associated with high cell densities of *G. catenatum* in the Gulf of California, Mexican Pacific coastline (Gárate-Lizárraga et al., 2005; Núñez-Vázquez et al., 2011). Moreover, approximately 10% of the > 2000 PSP cases in Southeast Asia related to human fatalities are believed to be caused by *P. bahamense* and *G. catenatum* (Lim et al., 2012; Furuya et al., 2018).

In our study, eight PST analogues were detected when *G. catenatum* cells were found in high abundances. The toxin profiles showed a similarity with PST components from strains found at the Pacific coast of Mexico, which were dominated by dcSTX, dcGTX2-3, C1 and C2 (Band-Schmidt et al., 2010). In addition, strains from the Portuguese coast showed similar profiles, however with additional C3-4, B1-2 and dcNEO (Costa et al., 2010; Costa et al., 2015). In contrast, Singapore and Yellow Sea (Korean coast line) *G. catenatum* clones revealed unique PST profiles, dominated by carbamoyl toxins (GTX1-4, NEO and STX), while no decarbamoyl and N-Sulfocarbamoyl toxins were detected

Table 3
Spearman rho correlations between biological parameters and environmental properties. Abbreviations: PTX2 (Pectenotoxin-2), PSTs (total PST level), DM (*Dinophysis miles*), AS (*Alexandrium* spp.), GC (*Gymnodinium catenatum*), Ts (temperature surface), Ta (temperature average 0–20 m), Ss (salinity surface), Sa (salinity average 0–20 m), MLD (mixed layer depth), kd (irradiance attenuation), P0 (phosphate 2 m), N0 (nitrate at surface 2 m), S0 (silicate 2 m), A0 (ammonium 2 m), P20 (phosphate 20 m), N20 (nitrate 20 m), S20 (silicate 20 m), A20 (ammonium 20 m), Chl-a net (chlorophyll-a ≥20 μm from the net).

Environmental factors	Overall year/annual					Wet season				
	PTX2	DM	PSTs	AS	GC	PTX2	DM	PSTs	AS	GC
DM	0.5**	–	–	–	–	0.30*	–	–	–	–
AS	–	–	0.43**	–	–	–	–	0.41**	–	–
GC	–	–	0.95**	–	–	–	–	0.67**	–	–
Ts	−0.37**	−0.37**	–	–	–	–	–	0.51**	0.48**	0.38**
Ta	−0.43**	−0.42**	–	−0.17*	−0.15*	–	–	0.61**	0.41**	0.39**
Ss	−0.21*	−0.32**	–	–	–	–	–	–	–	–
Sa			−0.34**	−0.23**	–	−0.26*	–	−0.45**	−0.48**	−0.20n
MLD	0.33**	0.34**	0.30**	0.30**	0.31*	–	–	–	–	–
Stratification	0.31**	0.51**	–	0.31**	–	–	–	–	0.28*	–
kd	0.40**	0.60**	–	0.30**	0.30**	0.30*	0.52**	–	–	–
Tide	0.44**	0.39**	0.30**	0.40**	0.26**	–	–	–	–	–
P0	−0.19*	–	–	–	–	–	–	–	0.27*	–
P20	–	0.24*	0.21*	–	–	–	0.43**	0.34**	0.39**	–
N0	0.22**	0.22*	–	0.23*	–	–	–	–	–	–
N20	0.24**	0.47**	0.20n	0.17n	–	–	0.43**	–	–	–
S0	0.30**	0.30**	–	–	–	–	–	−0.22	–	–
S20	0.30**	0.42**	–	0.20*	–	–	–	−0.30*	–	–
A0	0.25**	–	–	0.20*	–	–	–	−0.39*	−0.30*	−0.27*
A20	0.30**	–	–	0.22*	–	–	–	−0.33*	−0.29*	−0.20n
Chl-a	0.50**	0.40**	0.20*	0.41**	0.4**	–	–	–	–	0.2n
Precipitation	0.33**	0.34**	0.30**	0.30**	0.31**	–	–	–	–	–

** $p = 0.000$.
* $p < 0.01$.
n $p < 0.05$.

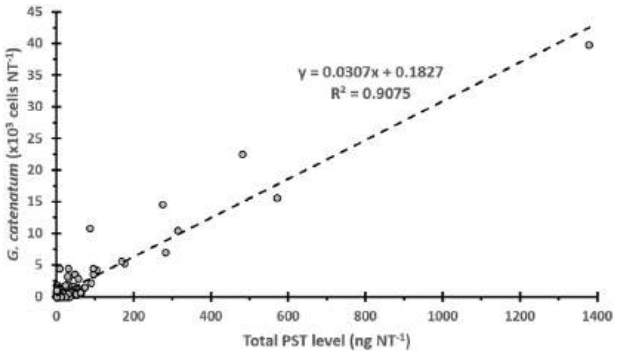

Fig. 8. Linear regression model of *Gymnodinium catenatum* cell abundance versus the total PST level.

(Holmes et al., 2002; Park et al., 2004). Although at low levels, the detection of carbamoyl toxins (GTX2-3 and STX) in our samples demonstrates that *G. catenatum* cells found in Ambon Bay are able to produce these highly toxic toxin analogues. The dominant N-Sulfocarbamoyl toxins of *G. catenatum* in our samples is likely to pose a high risk to seafood consumers due to the biotransformation of C-toxins to GTXs and B-toxins to STX & NEO in shellfish and other planktonic vectors (Krock et al., 2007).

Throughout the research, several physical properties such as MLD, irradiance attenuation and tidal elevation correlated with *G. catenatum*. Meanwhile, temperature was found as the main factor enhancing cell abundance and PST level during the wet season. Smayda (2002) found that this species is able to withstand various physical conditions including mixing due to its ability to increase swimming speed. This ecological strategy allows *G. catenatum* cells to migrate to different environments where light and nutrients are vertically separated (Doblin et al., 2006). Mexican and tropical strains from the Philippines and Thailand revealed a broad temperature tolerance for growth, and the maximum growth rate was found between 21 and 29 °C (reviewed by Hallegraeff et al., 2012). Moreover, the authors concluded that broad temperature tolerances might regulate *G. catenatum* seasonal and inter-annual bloom variations in natural waters. Besides influencing cell growth rate and density, temperature was also found to induce cell toxin profiles, in particular those of decarbamoyl and sulfocarbamoyl components (Band-Schmidt et al., 2014). Yet, in their study, no association was shown between cell toxicity levels and temperature.

Nutrient concentrations showed no clear correlations with both *G. catenatum* cell abundance and toxin level for the data of the whole sampling period. Yet, ammonium inversely correlated with cell abundance in the wet season. Bloom proportions of *G. catenatum* in Tasmanian waters (Australia) were generally observed during surface nitrate depletion (Doblin et al., 2006). Even though the species can migrate vertically to exploit nutrients at certain depths, *G. catenatum* is also known as a poor competitor for inorganic nutrient uptake such as nitrate, ammonium and phosphate (Yamamoto et al., 2004). Moreover, culture studies revealed unclear effects of nutrients on *G. catenatum* toxin content and toxin profiles (Flynn et al., 1996; Bustillos-Guzmán et al., 2012), yet N:P ratios were found to affect cell densities (Bustillos-Guzmán et al., 2012). Thus, the combination of migration ability and lack of competitive success may result in unclear correlations among *G. catenatum* abundance, toxin level and nutrient concentrations in field studies.

4.3. PTX2 and associated species

Three major *Dinophysis* species, *D. acuminata*, *D. caudata*, and *D. miles* were observed in Ambon Bay, of which all are known as potential DST and PTX producers. Interestingly, the three dominant species showed spatial distribution discrepancies, of which high *D. miles* abundances generally found in the inner bay and the two others in the outer station A. Yet, co-occurrence of these three species frequently recorded in samples from both parts of the bay. Taylor (1976) reported that *D. caudata* is a neritic species distributed in tropical and sub-tropical waters, while *D. acuminata* is a cosmopolitan coastal species

(reviewed by Reguera et al., 2014). Yet, blooms of *D. caudata* were observed co-occurring with other *Dinophysis* species including *D. acuminata* and *D. miles* (Marasigan et al., 2001; Reguera et al., 2012; Reguera et al., 2014).

Among the three dominant species, *D. miles* was the most abundant and showed a weak positive correlation with PTX2 levels, whereas no correlation was found for the other two *Dinophysis* species. In addition, this weak correlation between *D. miles* and PTX2 could be due to the fact that the three co-occurring species might contain differences in PTX2 cell quota. Furthermore, this might be due to non-synchronized peaks in toxin and *D. miles* levels, suggesting variability in toxin cell quota in response to environmental conditions and different growth stages, as found before for other *Dinophysis* species (Tong et al., 2011; Nielsen et al., 2012; Nielsen et al., 2013; Mafra et al., 2014; Basti et al., 2015; Ajani et al., 2016). PTX2 is the most abundant toxin produced by *Dinophysis* species, and commonly detected in *D. acuminata* and *D. caudata* (MacKenzie et al., 2005; Fernández et al., 2006; Krock et al., 2009; Basti et al., 2015; Fabro et al., 2016; Uchida et al., 2018). Meanwhile, the only study on a DSP event associated with *D. miles* was recorded for the Philippines. This study showed that the species produced OA and DTX1 only, with no PTX components being detected (Marasigan et al., 2001). Thus, our study is the first record of *D. miles* correlating with PTX2 in natural samples, while OA and its variants DTXs were not detected. Besides its occasional occurrences and low cell densities in plankton samples, the limited number of studies on *D. miles* may furthermore be due to its restricted distribution in some tropical areas (Marasigan et al., 2001; reviewed by Reguera et al., 2012), the Indo-West Pacific region (Arabian Sea, South China Sea and Indian Ocean) and the eastern Mediterranean (Reguera et al., 2014).

Throughout the research, PTX2 levels and *D. miles* cell abundances positively corresponded to nutrient (nitrate and silicate) concentrations and physical properties such as MLD, stratification, irradiance attenuation (kd) and tidal elevation, while being inversely correlated with temperature. Clearly, cell abundances and toxin levels were enhanced during the wet season and associated with relatively low temperature and reduced light availability (high kd indices). Nutrient availability at depth (phosphate and nitrate at 20 m) correlated with cell abundance, but not with toxin levels. Given the lack of knowledge on *D. miles* both in the field and in culture studies, information on growth response as a function of environmental drivers as well as (variability in) toxin quota is urgently needed.

As for the two other *Dinophysis* species, toxic *D. acuminata*, and *D. caudata* blooms were associated with seasons, nutrients, thermal stratification, salinity and dissolved oxygen in a south-eastern Australian estuary (Ajani et al., 2016). Various studies have shown unclear effects of temperature and irradiance on growth rate and toxin production of *Dinophysis* species (Pizarro et al., 2008; Fux et al., 2010; Tong et al., 2011; Nielsen et al., 2012; Mafra et al., 2014; Basti et al., 2015). Other field studies showed effects of water properties like upwelling- and sinking cycles, tides and stratification on *Dinophysis* density and toxin dynamics (Alves-de-Souza et al., 2014; Velo-Suárez et al., 2014).

5. Conclusions

Toxic dinoflagellate species persistently occur in Ambon Bay, exposing the area to potential shellfish poisoning events especially during the wet season. The total PST level shows a linear strong positive correlation with *G. catenatum* abundance. Moreover, the present data reveal the first record of *D. miles* association with PTX2 levels throughout the research. However, due to a lack of knowledge, culture studies on *D. miles* strains, isolated from the area, are required to confirm both toxin profile and variability. Associations with biological factors including the presence of grazers and bacteria, as well as species behaviour such as vertical migration were not addressed in our study, thus need attention in future studies. Finally, further research is needed to reveal toxin levels and profiles accumulated in shellfish and other marine biota, in order to fully understand the link between toxic dinoflagellate variability at the observed non-bloom conditions and food safety.

Supplementary data to this article can be found online at https://doi.org/10.1016/j.marpolbul.2019.110778.

Acknowledgements

We thank Willem M. Tatipatta and Eduard Moniharapon for operating the CTD, Malik S. Abdul for analyzing nutrients, Christophe Brochard for performing qualitative microscopic analysis, and Ronald Visser for preparing and setting up equipment in Ambon. Especially, we would like to thank Dr. Augy Syahailatua for allowing us to work in the LIPI's plankton laboratory during our campaign in Ambon. This work was supported and funded by LPDP program (Nomor: PRJ-1007/LPDP.3/2016), the Indonesian Ministry of Finance and partially funded by the Helmholtz-Gemeinschaft Deutscher Forschungszentren through the research program PACES II of the Alfred Wegener Institut-Helmholtz Zentrum für Polar- und Meeresforschung.

References

Aditya, V., Koswara, A., Fitriya, N., Rachman, A., Sidabutar, T., Thoha, H., 2013. Public awareness on Harmful Algal Bloom (HAB) in Lampung Bay. Mar. Res. Indones. 38 (2), 71–75.

Ajani, P., Larsson, M.E., Rubio, A., Bush, S., Brett, S., Farrell, H., 2016. Modelling bloom formation of the toxic dinoflagellates *Dinophysis acuminata* and *Dinophysis caudata* in a highly modified estuary, southeastern Australia. Estuar. Coast. Shelf Sci. 183, 95–106.

Alves-de-Souza, C., Varela, D., Contreras, C., de La Iglesia, P., Fernández, P., Hipp, B., Hernández, C., Riobó, P., Reguera, B., Franco, J.M., Diogène, J., García, C., Lagos, N., 2014. Seasonal variability of *Dinophysis* spp. and *Protoceratium reticulatum* associated to lipophilic shellfish toxins in a strongly stratified Chilean fjord. Deep-Sea Res. II Top. Stud. Oceanogr. 101, 152–162.

Anderson, D.M., 2009. Approaches to monitoring, control and management of harmful algal blooms (HABs). Ocean & Coastal Management 52 (7), 342–347.

Anderson, D.M., Couture, D.A., Kleindinst, J.L., Keafer, B.A., McGillicuddy Jr., D.J., Martin, J.L., Richlen, M.L., Hickey, J.M., Solow, A.R., 2014. Understanding interannual, decadal level variability in paralytic shellfish poisoning toxicity in the Gulf of Maine: the HAB Index. Deep-Sea Res. II Top. Stud. Oceanogr. 103, 264–276.

APHA, 1998. Standard Methods for the Examination of Water and Wastewater, 20th edition. American Public Health Association, American Water Works Association and Water Environmental Federation, Washington DC.

Band-Schmidt, C.J., Bustillos-Guzmán, J.J., López-Cortés, D.J., Gárate-Lizárraga, I., Núñez-Vázquez, E.J., Hernández-Sandoval, F.E., 2010. Ecological and physiological studies of *Gymnodinium catenatum* in the Mexican Pacific: a review. Marine drugs 8 (6), 1935–1961.

Band-Schmidt, C.J., Bustillos-Guzmán, J.J., Hernández-Sandoval, F.E., Núñez-Vázquez, E.J., López-Cortés, D.J., 2014. Effect of temperature on growth and paralytic toxin profiles in isolates of *Gymnodinium catenatum* (Dinophyceae) from the Pacific coast of Mexico. Toxicon 90, 199–212.

Basti, L., Uchida, H., Matsushima, R., Watanabe, R., Suzuki, T., Yamatogi, T., Nagai, S., 2015. Influence of temperature on growth and production of pectenotoxin-2 by a monoclonal culture of *Dinophysis caudata*. Marine drugs 13 (12), 7124–7137.

Blanco, J., Álvarez, G., Uribe, E., 2007. Identification of pectenotoxins in plankton, filter feeders, and isolated cells of a *Dinophysis acuminata* with an atypical toxin profile, from Chile. Toxicon 49 (5), 710–716.

Boëly, T., Gastellu-Etchegorry, J.P., Potier, M., Nurhakim, S., 1990. Seasonal and interannual variations of the sea surface temperatures (SST) in the Banda and Arafura Sea area. J. Sea Res. 25 (4), 425–429.

Burrell, S., Gunnarsson, T., Gunnarsson, K., Clarke, D., Turner, A.D., 2013. First detection of Paralytic Shellfish Poisoning (PSP) toxins in Icelandic mussels (*Mytilus edulis*): links to causative phytoplankton species. Food Control 31, 295–301.

Bustillos-Guzmán, J.J., Band-Schmidt, C.J., López-Cortés, D.J., Gárate-Lizárraga, I., Núñez-Vázquez, E.J., Hernández-Sandoval, F.E., 2012. Variations in growth and toxicity in *Gymnodinium catenatum* Graham from the Gulf of California under different ratios of nitrogen and phosphorus. Ciencias Marinas 38 (1A), 101–117.

Corvianawatie, C., Putri, M.R., Cahyarini, S.Y., Tatipatta, W.M., 2014. Variability of sea surface temperature and sea surface salinity in the Ambon Bay and its relation to ENSO/IOD and monsoon. Indonesian Journal of Geospatial 3 (2), 1–8.

Costa, P.R., Botelho, M.J., Lefebvre, K.A., 2010. Characterization of paralytic shellfish toxins in seawater and sardines (*Sardina pilchardus*) during blooms of *Gymnodinium catenatum*. Hydrobiologia 655 (1), 89–97.

Costa, P., Robertson, A., Quilliam, M., 2015. Toxin profile of *Gymnodinium catenatum* (Dinophyceae) from the Portuguese coast, as determined by liquid chromatography tandem mass spectrometry. Marine drugs 13 (4), 2046–2062.

Doblin, M.A., Thompson, P.A., Revill, A.T., Butler, E.C., Blackburn, S.I., Hallegraeff, G.M., 2006. Vertical migration of the toxic dinoflagellate *Gymnodinium catenatum* under different concentrations of nutrients and humic substances in culture. Harmful Algae 5 (6), 665–677.

Etheridge, S.M., 2010. Paralytic shellfish poisoning: seafood safety and human health perspectives. Toxicon 56, 108–122.
Fabro, E., Almandoz, G.O., Ferrario, M., Tillmann, U., Cembella, A., Krock, B., 2016. Distribution of *Dinophysis* species and their association with lipophilic phycotoxins in plankton from the Argentine Sea. Harmful Algae 59, 31–41.
Fernández, M.L., Reguera, B., González-Gil, S., Míguez, A., 2006. Pectenotoxin-2 in single-cell isolates of *Dinophysis caudata* and *Dinophysis acuta* from the Galician Rías (NW Spain). Toxicon 48 (5), 477–490.
Flynn, K.J., Flynn, K., John, E.H., Reguera, B., Reyero, M.L., Franco, J.M., 1996. Changes in toxins, intracellular and dissolved free amino acids of the toxic dinoflagellate *Gymnodinium catenatum* in response to changes in inorganic nutrients and salinity. J. Plankton Res. 18, 2093–2111.
Furuya, K., Iwataki, M., Lim, P.T., Lu, S., Leaw, C.P., Azanza, R.V., Kim, H.G., Fukuyo, Y., 2018. Overview of harmful algal blooms in Asia. In: Global Ecology and Oceanography of Harmful Algal Blooms, pp. 289–308.
Fux, E., González-Gil, S., Lunven, M., Gentien, P., Hess, P., 2010. Production of diarrhetic shellfish poisoning toxins and pectenotoxins at depths within and below the euphotic zone. Toxicon 56, 1487–1496.
Gárate-Lizárraga, I., Bustillos-Guzmán, J.J., Morquecho, L., Band-Schmidt, C.J., Alonso-Rodríguez, R., Erler, K., Lucas, B., Reyes-Salinas, A., Góngora-González, D.T., 2005. Comparative paralytic shellfish toxin profiles in the strains of *Gymnodinium catenatum* Graham from the Gulf of California, Mexico. Mar. Pollut. Bull. 50 (2), 211–217.
Glibert, P.M., 2016. Algal blooms. In: Encyclopedia of Estuaries, pp. 7–16.
González-Pola, C., Fernández-Díaz, J.M., Lavín, A., 2007. Vertical structure of the upper ocean from profiles fitted to physically consistent functional forms. Deep-Sea Res. I Oceanogr. Res. Pap. 54 (11), 1985–2004.
Hallegraeff, G.M., Fraga, S., 1996. Blooms dynamics of the toxic *Gymnodinium catenatum*, with emphasis on Tasmanian and Spanish coastal waters. In: Anderson, D., Cembella, A.D., Hallegraeff, G.H. (Eds.), Physiological Ecology of Harmful Algal Blooms. NATO ASI, Seriespp. 41 (59–80).
Hallegraeff, G.M., Blackburn, S.I., Doblin, M.A., Bolch, C.J.S., 2012. Global toxicology, ecophysiology and population relationships of the chain forming PST dinoflagellate *Gymnodinium catenatum*. Harmful Algae 14, 130–143.
Hess, P., 2010. Requirements for screening and confirmatory methods for the detection and quantification of marine biotoxins in end-product and official control. Anal. Bioanal. Chem. 397, 1683–1694.
Holmes, M.J., Bolch, C.J., Green, D.H., Cembella, A.D., Teo, S.L.M., 2002. Singapore isolates of the dinoflagellate *Gymnodinium catenatum* (Dinophyceae) produce a unique profile of paralytic shellfish poisoning toxins1. J. Phycol. 38 (1), 96–106.
Hu, T., LeBlanc, P., Burton, I.W., Walter, J.A., McCarron, P., Melanson, J.E., Strangman, W.K., Wright, J.L., 2017. Sulfated diesters of okadaic acid and DTX-1: self-protective precursors of diarrhetic shellfish poisoning (DSP) toxins. Harmful Algae 63, 85–93.
ICES, 2006. Report on the ICES/IOC Workshop on New and Classic Techniques for the Determination of Numerical Abundance and Biovolume of HAB Species – Evaluation of the Cost, Time-Efficiency and Intercalibration Methods (WKNCT), 22–27 August 2005, Kristineberg, Sweden. ICES CM (2005/C:10).
Ikhsani, I.Y., Abdul, M.S., Lekalette, J.D., 2016. Distribusi fosfat dan nitrat di Teluk Ambon bagian dalam pada musim barat dan timur. Widyariset 2 (2), 86–95 (in Indonesian, with English abstract).
James, K.J., Carey, B., O'halloran, J., van Pelt, F.N.A.M., Kova, Z.S., 2010. Shellfish toxicity: human health implications of marine algal toxins. Epidemiology & Infection 138, 927–940.
Krock, B., Seguel, C.G., Cembella, A.D., 2007. Toxin profile of *Alexandrium catenella* from the Chilean coast as determined by liquid chromatography with fluorescence detection and liquid chromatography coupled with tandem mass spectrometry. Harmful Algae 6 (5), 734–744.
Krock, B., Tillmann, U., John, U., Cembella, A.D., 2008. LC-MS/MS on board ship – tandem mass spectrometry in the search for phycotoxins and novel toxigenic plankton from the North Sea. Anal. Bioanal. Chem. 392, 797–803.
Krock, B., Seguel, C.G., Valderrama, K., Tillmann, U., 2009. Pectenotoxins and yessotoxin from Arica Bay, North Chile as determined by tandem mass spectrometry. Toxicon 54 (3), 364–367.
Laabir, M., Collos, Y., Masseret, E., Grzebyk, D., Abadie, E., Savar, V., Sibat, M., Amzil, Z., 2013. Influence of environmental factors on the paralytic shellfish toxin content and profile of *Alexandrium catenella* (Dinophyceae) isolated from the Mediterranean Sea. Marine drugs 11 (5), 1583–1601.
Li, X., Li, Z., Chen, J., Shi, Q., Zhang, R., Wang, S., Wang, X., 2014. Detection, occurrence and monthly variations of typical lipophilic marine toxins associated with diarrhetic shellfish poisoning in the coastal seawater of Qingdao City, China. Chemosphere 111, 560–567.
Likumahua, S., 2013. The recent bloom of *Pyrodinium bahamense* var. *compressum* in Ambon Bay, Eastern Indonesia. Mar. Res. Indones. 38 (1), 31–37.
Lim, P.T., Usup, G., Leaw, C.P., 2012. Harmful algal blooms in Malaysian waters. Sains Malays 41, 1509–1515.
Lindahl, O., Lundve, B., Johansen, M., 2007. Toxicity of *Dinophysis* spp. in relation to population density and environmental conditions on the Swedish west coast. Harmful Algae 6 (2), 218–231.
MacKenzie, L., Beuzenberg, V., Holland, P., McNabb, P., Suzuki, T., Selwood, A., 2005. Pectenotoxin and okadaic acid-based toxin profiles in *Dinophysis acuta* and *Dinophysis acuminata* from New Zealand. Harmful Algae 4 (1), 75–85.
Mafra, L.L., dos Santos Tavares, C.P., Schramm, M.A., 2014. Diarrheic toxins in field-sampled and cultivated *Dinophysis* spp. cells from southern Brazil. J. Appl. Phycol. 26 (4), 1727–1739.
Marasigan, A.N., Sato, S., Fukuyo, Y., Kodama, M., 2001. Accumulation of a high level of diarrhetic shellfish toxins in the green mussel *Perna viridis* during a bloom of *Dinophysis caudata* and *Dinophysis miles* in Sapian Bay, Panay Island, the Philippines. Fish. Sci. 67 (5), 994–996.
Miles, C.O., Wilkins, A.L., Hawkes, A.D., Jensen, D.J., Cooney, J.M., Larsen, K., Petersen, D., Rise, F., Beuzenberg, V., MacKenzie, A.L., 2006. Isolation and identification of a cis-C8-diol-ester of okadaic acid from *Dinophysis acuta* in New Zealand. Toxicon 48 (2), 195–203.
Navarro, J.M., Gonzalez, K., Cisternas, B., Lopez, J.A., Chaparro, O.R., 2014. Contrasting physiological responses of two populations of the razor clam *Tagelus dombeii* with different histories of exposure to Paralytic Shellfish Poisoning (PSP). PLoS One 9 (8), e105794. https://doi.org/10.1371/journal.pone.0105794.
Nielsen, L.T., Krock, B., Hansen, P.J., 2012. Effects of light and food availability on toxin production, growth and photosynthesis in *Dinophysis acuminata*. Mar. Ecol. Prog. Ser. 471, 37–50.
Nielsen, L.T., Krock, B., Hansen, P.J., 2013. Production and excretion of okadaic acid, pectenotoxin-2 and a novel dinophysistoxin from the DSP-causing marine dinoflagellate *Dinophysis acuta*–effects of light, food availability and growth phase. Harmful Algae 23, 34–45.
Núñez-Vázquez, E.J., Gárate-Lizarraga, I., Band-Schmidt, C.J., Cordero-Tapia, A., Lopez-Cortes, D.J., Sandoval, F.E.H., Heredia-Tapia, A., Bustillos-Guzmán, J.J., 2011. Impact of harmful algal blooms on wild and cultured animals in the Gulf of California. J. Environ. Biol. 32 (4), 413.
Park, T.G., Kim, C.H., Oshima, Y., 2004. Paralytic shellfish toxin profiles of different geographic populations of *Gymnodinium catenatum* (Dinophyceae) in Korean coastal waters. Phycol. Res. 52 (3), 300–305.
Pizarro, G., Escalera, L., González-Gil, S., Franco, J.M., Reguera, B., 2008. Growth, behaviour and cell toxin quota of *Dinophysis acuta* during a daily cycle. Mar. Ecol. Prog. Ser. 353, 89–105.
Pizarro, G., Paz, B., González-Gil, S., Franco, J.M., Reguera, B., 2009. Seasonal variability of lipophilic toxins during a *Dinophysis acuta* bloom in Western Iberia: differences between picked cells and plankton concentrates. Harmful Algae 8 (6), 926–937.
Reguera, B., Velo-Suárez, L., Raine, R., Park, M.G., 2012. Harmful *Dinophysis* species: a review. Harmful Algae 14, 87–106.
Reguera, B., Riobó, P., Rodríguez, F., Díaz, P., Pizarro, G., Paz, B., Franco, J.M., Blanco, J., 2014. *Dinophysis* toxins: causative organisms, distribution and fate in shellfish. Marine Drugs 12 (1), 394–461.
Reis Costa, P., 2016. Impact and effects of paralytic shellfish poisoning toxins derived from harmful algal blooms to marine fish. Fish Fish. 17 (1), 226–248.
Saputra, F.R.T., Lekalette, J.D., 2016. Dinamika masa air di Teluk Ambon. Widyariset 2 (2), 143–152 (in Indonesian, with English abstract).
Smayda, T.J., 2002. Turbulence, watermass stratification and harmful algal blooms: an alternative view and frontal zones as pelagic seed banks. Harmful Algae 1, 95–112.
Somavilla, R., González-Pola, C., Fernández-Diaz, J., 2017. The warmer the ocean surface, the shallower the mixed layer. How much of this is true? Journal of Geophysical Research: Oceans 122 (9), 7698–7716.
Strickland, J.D., Parsons, T.R., 1972. A Practical Handbook of Seawater Analysis. The Alger Press Ltd.
Suzuki, T., Miyazono, A., Baba, K., Sugawara, R., Kamiyama, T., 2009. LC–MS/MS analysis of okadaic acid analogues and other lipophilic toxins in single-cell isolates of several *Dinophysis* species collected in Hokkaido, Japan. Harmful Algae 8 (2), 233–238.
Tatters, A.O., Flewelling, L.J., Fu, F., Granholm, A.A., Hutchins, D.A., 2013. High CO_2 promotes the production of paralytic shellfish poisoning toxins by *Alexandrium catenella* from Southern California waters. Harmful Algae 30, 37–43.
Taylor, F.J.R., 1976. Dinoflagellates from the International Indian Ocean Expedition; A Report of the Material Collected by the R.V. —AntonBruun‖ 1963–1964. Bilbliotheca Botanica, Stuttgart, Germany, pp. 234.
Tong, M., Kulis, D.M., Fux, E., Smith, J.L., Hess, P., Zhou, Q., Anderson, D.M., 2011. The effects of growth phase and light intensity on toxin production by *Dinophysis acuminata* from the northeastern United States. Harmful Algae 10, 254–264.
Uchida, H., Watanabe, R., Matsushima, R., Oikawa, H., Nagai, S., Kamiyama, T., Baba, K., Miyazono, A., Kosaka, Y., Kaga, S., Matsuyama, Y., Suzuki, T., 2018. Toxin profiles of okadaic acid analogues and other lipophilic toxins in *Dinophysis* from Japanese coastal waters. Toxins 10 (11), 457.
Ujevic, I., Rojeb, R., Nincevic-Gladan, Z., Marasovi, I., 2012. First report of paralytic shellfish poisoning (PSP) in mussels (*Mytilus galloprovincialis*) from eastern Adriatic Sea (Croatia). Food Control 25, 285–291.
Velo-Suárez, L., González-Gil, S., Pazos, Y., Reguera, B., 2014. The growth season of *Dinophysis acuminata* in an upwelling system embayment: a conceptual model based on in situ measurements. Deep-Sea Res. II Top. Stud. Oceanogr. 101, 141–151.
Wagey, G.A., 2002. Ecology and Physiology of Phytoplankton in Ambon Bay, Indonesia (Doctoral dissertation). University of British Columbia.
Wiadnyana, N.N., Sidabutar, T., Matsuoka, K., Ochi, T., Kodama, M., Fukuyo, Y., 1996. Note on the occurrence of *Pyrodinium bahamense* in eastern Indonesian waters. In: Yasumoto, T., Oshima, Y., Fukuyo, Y. (Eds.), Harmful and Toxic Algal Blooms. IOC/UNESCO Paris, pp. 53–56.
Wyrtki, K., 1961. Physical Oceanography of the Southeast Asian Waters. (California).
Xie, W., Liu, X., Yang, X., Zhang, C., Bian, Z., 2013. Accumulation and depuration of paralytic shellfish poisoning toxins in the oyster *Ostreari vularis* Gould e chitosan facilitates the toxin depuration. Food Control 30, 446–452.
Yamamoto, T., Oh, S.J., Kataoka, Y., 2004. Growth and uptake kinetics for nitrate, ammonium and phosphate by the toxic dinoflagellate *Gymnodinium catenatum* isolate from Hiroshima Bay, Japan. Fish. Sci. 70, 108–115.
Zijlstra, J.J., Baars, M.A., Tijssen, S.B., Wetsteyn, F.J., Witte, J.I., Ilahude, A.G., 1990. Monsoonal effects on the hydrography of the upper waters (< 300 m) of the eastern Banda Sea and northern Arafura Sea, with special reference to vertical transport processes. J. Sea Res. 25 (4), 431–447.